

Military Technical College
Kobry El-Kobbah,
Cairo, Egypt.



13th International Conference
on Applied Mechanics and
Mechanical Engineering.

SIMULATION AND OPTIMIZATION OF H₂O-LIBR ABSORPTION REFRIGERATION SYSTEM OPERATED BY SOLAR ENERGY UNDER EGYPTIAN CLIMATIC CONDITIONS

FATOUH^{*} M. HASSAN^{**} M. and Abdel Dayem^{***} A.M.

ABSTRACT

Among various types of clean energies, special attention has given to a solar energy because it is freely available in hot regions where more than half the world's population lives. Use of solar energy in vapor absorption refrigeration systems should be one application which can achieve cooling/heating needs. In general, solar cooling systems can be considered as combination of energy conversion and refrigeration subsystems. The energy conversion subsystem transforms solar energy to power the refrigeration system. In the present work, a solar cooling system for air conditioning applications is simulated and optimized under Egyptian meteorological conditions. According to the required comfort dry bulb air temperature, available cooling water temperature and cooling coil capacity, optimal heat source mass flow rate and temperature to operate a single-stage continuous absorption cycle was obtained. Then, economical optimization of the solar system that can meet the required load was carried out for various types of solar collectors. Results revealed that the flat-plate solar collector is the most efficient collector from the economical point of view. Annual visualization of the system performance was presented to investigate the system behavior under different weather conditions for heating and cooling processes during the year to improve its life-cycle savings. The environmental impact of using such system is considered. It is found that the reduction of CO₂ emission is a significant advantage of using solar energy.

KEY WORD

Solar, Cooling, Absorption, Single Effect, Simulation, Collector, and Environmental Impact.

* Professor, Dpt. of Mech. Power Eng., Helwan University, Cairo, Egypt.

** Lecturer, Dpt. of Mech. Power Eng., Helwan University, Cairo, Egypt.

*** Associate Professor, Dpt. of Mech. Power Eng., Helwan University, Cairo, Egypt.

NOMENCLATURE

A	total collector array aperture or gross, m ²
A _i	surface area of the ith tank segment, m ²
b ₀	negative of the first-order coefficient of $(\tau\alpha)_b/(\tau\alpha)_n$ vs. $(I/\cos\theta - I)$
b ₁	negative of the second-order coefficient of $\tau\alpha)_b/(\tau\alpha)_n$ vs. $(I/\cos\theta - I)$
c _A	collector price, US\$/m ²
c _f	fuel price, US\$/GJ (12 L.E./GJ is considered)
C _M	price of the storage tank, US\$/kg
C _{pc}	specific heat of collector fluid, kJ/kg.C
C _p	specific heat, kJ/kg.C
C _{pf}	specific heat of the tank fluid, kJ/kg.C
c _o	fixed cost of the system, US\$
COP	coefficient of performance
F _R	overall collector heat removal efficiency factor
F _R U _L	negative of the first-order coefficient of collector efficiency vs $(T_i - T_a)/I_T$
F _R U _L	combined first and second-order coefficients of collector efficiency vs $(T_i - T_a)/I_T$
F'	collector fin efficiency factor
F _{par}	fraction of pump/fan power converted to fluid thermal energy
h	enthalpy, J/kg
g _i	flag for boundary segments
G _{test}	flow rate per unit area at test conditions, kg/m ²
h	specific enthalpy, kJ/kg
I	total horizontal radiation per unit area, W/m ²
I _{bT}	incident beam radiation per unit area on tilted surfaces, W/m ²
I _d	horizontal diffuse radiation per unit area, W/m ²
I _T	total incident radiation on a tilted flat surface per unit area, W/m ²
L.S.	life cycle solar savings, US\$
M	mass of the storage tank, kg.
m	mass flow rate, kg/s
m _c	collector mass flow rate, kg/s
M _i	mass of fluid in the ith section inside the tank, kg
N	lifetime of the system, yr. (20 years is expected).
O _M	annual charge for operation and maintenance of the system expressed as a fraction of capital cost (2% is assumed).
P	power consumption of pump, W
Q	rate of heat transfer, W
Q _i	rate of energy input by the heating element to the tank ith segment, W
Q _u	rate of energy gain of total collector array, W
r	Real rate of return on alternative investments of comparable risk.
r _f	real fuel escalation rate.
r ₁	factor for correcting F _R ($\tau\alpha$) _n and F _R U _L ' for operation at flow rates other than that at test conditions
T	Temperature, °C
T _a	ambient temperature, °C
T _{env}	temperature of the environment surrounding the tank, °C

T_i inlet temperature of fluid or temperature of the i th tank segment, °C
 U_L overall loss coefficient of collector per unit aperture area, W/m².C

Subscripts

1-10	refer to Fig. (2)	i	inlet
abs	absorber	L	load side
con	condense	n	normal
e	evaporator	o	outlet
h	hot or heat-exchanger	ref	reference
g	generator	s	surface or solution
j	segment number		

Symbols

α absorptance of absorber plate
 α_i a control function defined by
 $\alpha_i = 1$ if $i = S_h$; 0 otherwise
 β collector slope (in degrees)
 β_i a control function defined by
 $\beta_i = 1$ if $i = S_L$; 0 otherwise
 Δt simulation time step, s
 η overall collector efficiency
 η_{backup} boiler backup efficiency (75% is normally considered).
 γ_i a control function defined by

$$\gamma_i = \dot{m}_h \sum_{j=1}^{i-1} \alpha_j - \dot{m}_L \sum_{j=i+1}^N \beta_j$$
 θ solar incidence angle (degree)
 ρ_g ground reflectance
 τ transmittance of collector cover

INTRODUCTION

There are only two mechanical air-conditioning chillers have been extensively used in various applications. They are vapor compression chillers and vapor absorption chillers. Vapor absorption chiller is principally similar to the well known vapor compression chiller in that it uses a refrigerant which alternatively evaporates at low pressure and condenses at high pressure. The main difference between the two chillers is the driving force that circulates the refrigerant around the system. In the absorption chiller, compressor is replaced with an absorber, circulation pump, expansion device and generator. Another difference is that the energy input to the absorption chiller is mainly of heat supplied to the generator. Hence, low-grade energy such as a solar energy can be used to operate vapor absorption refrigeration systems to achieve cooling needs.

In general, solar cooling systems can be viewed as combinations of energy conversion and refrigeration subsystems. The energy conversion subsystem transforms solar energy to power the vapor absorption refrigeration system. Therefore, solar absorption

cooling can obtain a great potential because it is used during the summer months when they have long day time and higher ambient temperature.

Many investigators have developed computer programs or mathematical models to predict performance characteristics of vapor absorption chillers. Investigations on the effect of various operating conditions form a part of such studies with the aim of providing basic information for design of absorption chillers working with different refrigerant-absorbent pairs. In this work, the emphasis is on presentably commercially water lithium bromide based vapor absorption chillers for air-conditioning applications. This is due many advantages of this working fluid such as high heat of vaporization, non-toxic, non-flammable, availability, inexpensive ... etc.

Romero et al. (2000) compared the theoretical performance of a solar absorption air conditioning system operating with water/lithium bromide and an aqueous ternary hydroxide mixture consisting of sodium, potassium and cesium hydroxides. The results showed that similar coefficients of performance are obtained for both mixtures. However, it was found that the system operating with the hydroxides may operate with a higher range of condenser and absorber temperatures and the heat delivered by these components can be removed by air. Li and Sumathy (2000) reviewed solar powered air-conditioning systems using water-lithium bromide pair. It is seen that the generator inlet temperature of the chiller is the most important parameter in the design and fabrication of a solar powered air-conditioning system.

Performance evaluation of single-glazed and double-glazed collectors for an open-cycle absorption solar cooling system is conducted by YANG and WANG (2001) for air-conditioning applications in Kaohsiung, Taiwan via a computer simulation program. It is shown that the double glazed forced convection gives a better system performance. Simulation of an absorption solar cooling system under Cyprus climatic conditions is presented by Florides et al. (2002). Their system operates with maximum performance when the auxiliary boiler thermostat is set at 87°C. The system long-term integrated performance shows that cooling load of 84,240 MJ and heating load of 41,263 MJ are supplied with solar energy. Tsoutsos et al. (2003) developed an economic evaluation of two types of solar absorption and adsorption cooling systems. Their analyses indicated that, because of their high investment cost, these systems would be marginally competitive with compression cooling systems at present energy prices.

Assilzadeh et al. (2005) simulated a solar cooling system, which consists of evacuated tube solar collectors and water-lithium bromide absorption refrigeration unit. The optimum solar subsystem for Malaysia's climate for a cooling capacity of 3.5 kW (1 refrigeration ton) consists of 35 m² evacuated tubes solar collector sloped at 20°. Water-lithium bromide absorption refrigeration system is simulated and optimized by Balghouthi et al. (2005) for Tunisian conditions. The simulation results show that absorption solar air conditioning systems are suitable for Tunisian's conditions. Syed et al. (2005) reported novel experimental results derived through field testing of a part load solar energized cooling system for typical Spanish houses in Madrid during the summer period of 2003. Solar insolation of 969 W m² produced 5.13 kW of cooling at a solar to cooling conversion efficiency of 11%. Maximum cooling capacity was 7.5 kW. The absorption refrigeration machine operated within the generation and absorption temperature ranges of 57–67 and 32–36 °C, respectively. The results clearly

demonstrate that the technology works best in dry and hot climatic conditions where large daily variations in relative humidity and dry bulb temperature prevail.

From the above investigations, the solar absorption cooling has more current interest from the researchers. The studies tend to improve the performance numerically by considering many parameters. Therefore this work considers the parameters that have a significant effect on the solar absorption system performance. Computer modeling of thermal systems presents many advantages. The most important are the elimination of the expense of building prototypes, the optimization of the system components, estimation of the amount of energy delivered from the system, and prediction of temperature variations of the system. Optimization of the solar system and absorption cycle is developed. Accordingly solar collectors are compared with different specifications. TNSYS program is used to carry out the numerical simulation.

MATHEMATICAL MODEL

The numerical simulation was developed using the software of TRNSYS 15, the details of the program is presented in the manual of the program [see Ref. 11]. TRNSYS is a transient system simulation program with a modular structure. A system is defined in TRNSYS to be a set of components, interconnected in such a manner as to accomplish a specified task. The software consists of different subroutines and each subroutine simulates a component of the solar system. For example, the present solar water-heating system may consist of a solar collector, energy storage units, an auxiliary energy heater, pipes, pumps and several temperature-sensing controllers. One obvious characteristic of a system is its modularity. Because the system consists of components, it is possible to simulate the performance of the system by collectively simulating the performance of the interconnected components.

A solar cooling system consists of solar and refrigeration subsystems. The solar system provides a heat to a generator of a single effect lithium bromide absorption cycle. As shown in Fig.1, the solar system contains a collector connected to a storage tank. A circulating pump-1 is used to control the flow rate of the solar loop by a control unit-1 through the collector temperature. The hot water from the tank is pumped (by pump-2) into the generator of the absorption cycle, a control unit-2 switches the pump. An off/on switched auxiliary heater is connected to the tank/load outlet to raise the lower temperature into the generator temperature. The return water from the absorption cycle is re-circulated through either the tank or directly to the auxiliary using either water mixer or diverter. The following subsections simulate the system components.

Solar Collector

Four collectors are considered to find the most appropriate collector. They are flat-plate, parabolic trough, compound parabolic concentrator and evacuated-tube collectors. This component models the thermal performance of various collector types [as described in Duffie and Beckman, 1991]. The total collector array may consist of collectors connected in series and in parallel. The thermal performance of the total collector array is determined by the number of modules in series and the characteristics of each module. A general expression for collector efficiency can be obtained from the Hottel-Whillier equation as

$$\eta = \frac{Q_u}{AI_T} = F_R(\tau\alpha) - F_R U_L \frac{(T_i - T_a)}{I_T} \quad (1)$$

In order to account for conditions when the collector is operated at a flow rate other than the value at which it was tested, both $F_R(\tau\alpha)_n$ and $F_R U_L'$ are corrected to account for changes in F_R . The ratio, r_1 , by which they are corrected as given by:

$$r_1 = \frac{\frac{\dot{m}_c C_{pc}}{AF'U_L} (1 - e^{-AF'U_L/\dot{m}_c C_{pc}}) \Big|_{use}}{\frac{G_{test} C_{pc}}{F'U_L} (1 - e^{-F'U_L/G_{test} C_{pc}})} \quad (2)$$

The parameter $F'U_L$ is considered to be flow rate independent and is calculated using the test flow rate as

$$F'U_L = -G_{test} \cdot C_{pc} \ln \left(1 - \frac{F_R U_L'}{G_{test} \cdot C_{pc}} \right) \quad (3)$$

Collector tests are generally performed on clear days at normal incidence so that the transmittance - absorptance product is nearly the normal incidence value for beam radiation, $(\tau\alpha)_n$. The intercept efficiency, $F_R(\tau\alpha)_n$, is corrected for non-normal solar incidence by the factor $(\tau\alpha)/(\tau\alpha)_n$. By definition, $(\tau\alpha)$ is the ratio of the total absorbed radiation to the incident radiation. Thus, a general expression for $(\tau\alpha)/(\tau\alpha)_n$ is

$$\frac{(\tau\alpha)}{(\tau\alpha)_n} = \frac{I_b \Gamma \frac{(\tau\alpha)_b}{(\tau\alpha)_n} + I_d \left(\frac{1 + \cos\beta}{2} \right) \frac{(\tau\alpha)_s}{(\tau\alpha)_n} + \rho_g I \left(\frac{1 - \cos\beta}{2} \right) \frac{(\tau\alpha)_g}{(\tau\alpha)_n}}{I_T} \quad (4)$$

For flat-plate collectors, $(\tau\alpha)_b/(\tau\alpha)_n$ can be approximated from ASHRAE test results (Hewett, 1991) as

$$\frac{(\tau\alpha)_b}{(\tau\alpha)_n} = 1 - b_0 \left(\frac{1}{\cos\theta} - 1 \right) - b_1 \left(\frac{1}{\cos\theta} - 1 \right)^2 \quad (5)$$

Stratified Fluid Storage Tank

The tank is divided into various segments. It is assumed that the fluid streams flowing up and down from each node are fully mixed before they enter each segment. An energy balance written about the i th tank segment is expressed as:

$$M_i C_{pf} \frac{dT_i}{dt} = \alpha_i \dot{m}_h C_{pf} (T_h - T_i) + \beta_i \dot{m}_L C_{pf} (T_L - T_i) + U A_i (T_{env} - T_i) + \gamma_i (T_{i-1} - T_i) C_{pf} \quad \text{If } g_i > 0$$

$$+ \gamma_i (T_i - T_{i+1}) C_{pf} \quad \text{If } g_i < 0$$

$$+ \dot{Q}_i \quad \text{For } i = 1, N \quad (6)$$

The temperatures of each of the N tank segments are determined by the integration of their time derivatives expressed in the above equation. At the end of each time step, temperature inversions are eliminated by mixing appropriate adjacent nodes.

Pump

This pump model computes a mass flow rate using a variable control function, which must be between 0 and 1, and a fixed (user specified) maximum flow capacity. Pump power consumption may also be calculated as a linear function of mass flow rate.

$$T_o = T_i + \frac{P * f_{par}}{\dot{m} C_p} \quad (7)$$

Pipe

This component models the thermal behavior of fluid flow in a pipe using variable size segments of fluid. Entering fluid shifts the position of existing segments. The mass of

the new segment (M_j) is equal to the flow rate (\dot{m}) times the simulation timestep (Δt). The new segment's temperature (T_j) is that of the incoming fluid (T_k). The outlet of this pipe is a collection of the elements that are "pushed" out by the inlet flow. This "plug-flow" model does not consider mixing or conduction between adjacent elements. The average outlet temperature is computed as the mass weighted average of leaving elements. In general:

$$T_o = \frac{1}{\dot{m}\Delta t} \left(\sum_{j=1}^{k-1} M_j T_j + a M_k T_k \right) \quad (8)$$

where a and k must satisfy $0 \leq a \leq 1$

$$\sum_{j=1}^{k-1} M_j + a M_k = \dot{m}\Delta t \quad (9)$$

Energy losses are considered for each element by solution of the following differential equation

$$M_j C_p \frac{dT_j}{dt} = -(UA)_j (T_j - T_{env}) \quad (10)$$

On/Off Differential Controller

This controller generates a control function γ_o that can have values of 0 or 1. The value of γ_o is chosen as a function of the difference between upper and lower temperatures, TH and TL, compared with two dead band temperature differences, ΔTH and ΔTL . The new value of γ_o is dependent on whether initial value $\gamma_i = 0$ or 1. The controller is normally used with γ_o connected to γ_i giving a hysteresis effect. For safety considerations, a high limit cut-out is included with the controller. Regardless of the

dead band conditions, the control function will be set to zero if the high limit condition is exceeded.

Economic Analysis

The optimal system that is considered in this study has the maximum payback payment during the lifetime (20 years). That means, this system is more efficient and its principle cost is relatively low. Duffie and Beckman [1991] and Gordon and Rabl [1982] discuss this method of optimization, which is based on the life-cycle savings (payback investment) of the system. This method is taken into consideration in this work.

The optimization is based on three factors. The first factor is the life-cycle savings (L.S.), which is defined as the difference between fuel savings and the cost of the capital, operation and maintenance [Gordon and Rabl]:

$$L.S. = q_u \cdot C_{f,l} - C_{cap} (c_o + c_A \cdot A + c_M \cdot M), \quad (11)$$

$$C_{f,l} = \frac{c_f (1+r_f)}{\eta_{backup} (r-r_f)} \left[1 - \left[\frac{1+r_f}{1+r} \right]^N \right] \quad (12)$$

and

$$C_{cap} = 1 + \frac{O_M}{r} [1 - (1+r)^{-N}]. \quad (13)$$

The second factor is the solar fraction defined as the ratio between the useful output energy of the solar energy system into the process heat and the required load energy.

$$SolarFraction = \frac{SystemOutputEnergy}{LoadEnergy}$$

The third effective factor in the comparison between the two systems is the system efficiency, the ratio between the output energy of the solar energy system to the input solar energy into the system:

$$SystemEfficiency = \frac{SystemOutputEnergy}{InputSolarEnergy}$$

Single-Effect Absorption Cycle

A schematic diagram of a single-effect continuous vapor absorption refrigeration system (VARS) is shown in Fig. 2. It essentially consists of the following main component: generator, absorber, condenser and evaporator, a solution heat exchanger, a solution pump and expansion valves. Water–lithium bromide is used as working fluid in the VARS. Liquid refrigerant receives heat (cooling load) in evaporator and vaporizes. This refrigerant vapor then flows to the absorber to be absorbed by strong solution in absorbent (mass fraction X_{ss}) which is returned from the generator, forming a weak solution in absorbent (mass fraction X_{ws}). The latter is pumped back to the generator where it is heated to release the refrigerant vapor, which is condensed in the

condenser. This condensate flows through an expansion device to the evaporator. Meanwhile, the strong solution from the generator returns to the absorber completing the cycle. The heat rejected at absorber and condenser is dissipated to the cooling water which is cooled via a cooling tower. Function of the solution heat exchanger is to recover the sensible heat of the solution flowing from the generator to the absorber. Thus, the strong solution flowing to the absorber is pre-cooled to increase its absorption capacity and to lessen the load on the cooling water. Also, the weak solution from the absorber is preheated to reduce the energy-input required at the generator. Therefore, the solution heat exchanger plays a crucial role in the performance of a VARS.

Energy balance is done for each component to calculate its load as given under here.

-Cooling load at evaporator.

$$Q_e = m_{ref}(h_{10}-h_8) \quad (14)$$

-The heat rejected in the condenser.

$$Q_{con} = m_{ref}(h_7-h_8) \quad (15)$$

-The heat rejected in the absorber.

$$Q_{abs} = m_{10}h_{10}+m_6h_6-m_1h_1=m_{ref}(h_{10}-h_6)+m_{ss}(h_6-h_1) \quad (16)$$

-The heat input to the generator.

$$Q_g = m_7h_7+m_4h_4-m_3h_3=m_{ref}(h_7-h_3)+m_{ss}(h_4-h_3) = m_{hs} c_{hs} \Delta T_{hs} \quad (17)$$

-Heat exchange in solution heat exchanger.

$$Q_h = m_{ss}(h_4-h_5)=m_{ws}(h_3-h_2) \quad (18)$$

Thermodynamic coefficient of performance $(COP)_{th}$ of vapor absorption refrigeration cycle is defined as the ratio of cooling capacity at evaporator and power consumption at generator and solution pump, i.e.

$$(COP)_{th} = Q_e / (Q_g + P_{sp}) \quad (19)$$

where Q_e is the cooling capacity, Q_g is the rate of heat transfer to generator and P_{sp} is the power of solution pump. The energy consumed by the solution pump is small in comparison with the energy supplied in the generator and following approximation is possible:

$$(COP)_{th} = Q_e / Q_g \quad (20)$$

The above components are interconnected together to estimate the different outputs. The hourly measured metrological data of Cairo 30 °N were used as an input. The data includes the total and diffuse solar radiation and the ambient temperature.

The above governing equations were solved together to find the different variables included in them. The unknown variables include the temperatures and flow rates at the inlets and outlets of each component. Moreover, the useful heat gain and heat losses

can be estimated that are the inputs of the economic analysis. In the following sections the results of the simulation are discussed.

RESULTS AND DISCUSSIONS

Optimization of the Single-Effect Absorption Cycle

Coefficient of performance (COP) of a single-effect vapor absorption refrigeration system (VARS) as a function of generator temperature is shown in Fig. 3. It is clear that COP increases with generator temperature when other operating parameters are kept constant. It is evident from this figure that optimal generator temperature is nearly 94°C which yields maximum COP. Figure 4 illustrates the variation of heat source water mass flow rate with generator temperature. Clearly, heat source water mass flow rate decreases then increases when generator temperature increases. Figure 4 reveals that optimal heat source water mass flow rate is obtained at generator temperature of about 94°C. Figures 3 and 4 confirm that the highest COP and lowest heat source water mass flow rate can be achieved at generator temperature of 94°C. Thus, heat source temperature and mass flow rate of 94°C and 0.07224 kg/s are considered as input parameters to optimize the solar energy subsystem.

Optimization of the Collector Area

An economical optimization is established to find the most economic collector. Four different collectors are considered; parabolic trough, flat-plate, evacuated-tube and compound parabolic concentrating collectors. The life-cycle savings, solar fraction and system efficiency are estimated as indicated in subsection 2.6. The considered specifications of each collector are as follows:

1. Parabolic-trough collector

Single glass cover, horizontal-axis tracking, $F_R U_L = 15$, $F_{RT\alpha} = 0.7$, concentration ratio = 35, no. of collectors in series = 1, no. of collectors in parallel = 1, price = 230 US\$/m², and tested flow rate = 50 kg/(hr.m²)

2. Flat-plate collector

Single glass cover, $F_R U_L = 15$, $F_{RT\alpha} = 0.7$, no. of collectors in series = 1, no. of collectors in parallel = 1, price = 75 US\$/m², and tested flow rate = 50 kg/(hr.m²)

3. Evacuated-tube collector

Single glass cover, $F_R U_L = 0.8$, $F_{RT\alpha} = 0.7$, concentration ratio = 35, no. of collectors in series = 1, no. of collectors in parallel = 1, price = 100 US\$/m², and tested flow rate = 3 kg/(hr.m²).

4. Compound parabolic concentrating collector (CPC)

Single glass cover, vertical axis tracking, $U_L = 3$, collector efficiency factor = 0.7, wall reflectivity = 0.9, truncation ratio = 0.7, half-acceptance angle = 45, no. of collectors in series = 1, price = 250 US\$/m², and no. of collectors in parallel = 1.

The year is divided into three seasons. The heating seasons are from January 1st to May 31 and from October 1st to December 31. The cooling season is generally considered from June 1st to September 30. It is found that the optimal collector flow rate that gives maximum energy gain from the collector is 25 kg/(hr.m²). It is used for each collector and changed with the surface area of it. The standard tank volume is used and it is about 75 liter per quadratic meter of the collector. The load of one kW power is considered in the study and the all results are estimated for that value for the cooling and heating load. The heating temperature required for the absorption-cycle generator is found to be 94 °C with temperature drop of 5 C through it and 260.02 kg/hr flow rate. Therefore, the load flow rate is estimated as 260 kg/hr for cooling in the period from June 1st to September 30 where it is found of 172.25 kg/hr for the heating load from January 1st to May 31 and from October 1st to December 31 with heating temperature of 60 °C. The three periods of time are normally defined for cooling and heating for Egypt weather.

The life-cycle savings (L.S.) are estimated for the system containing each collector as shown in the figures from Fig. 4 to Fig. 7. Perhaps the concentrating collectors, PTC and CPC, produce more energy than the others as indicated by the higher solar fraction (S.F.) as in Fig. 5 and Fig. 8, they have lower life payback. That is because their initial cost is high especially for the tracking systems. Therefore the flat-plate collector system gives the highest life-cycle savings as shown in Fig. 5 due to its lower price and simplicity.

From Fig. 6, it is found that the flat-plate collector is the most efficient from the economic point of view. The optimal collector area that is the most economic is 20 m² with 27% solar fraction. The flow rate of the collector is about 500 kg/hr and tank volume is 1500 liters.

Both PTC and evacuated tube collectors have negative values of life-cycle savings for any collector area as shown in the figure 5 and 7. Although they can cover a percentage of the required load but the collectors payback can not meet the high price of them. The CPC is better than them where it can produce positive life-cycle savings up to 12 m² collector area as presented in Fig. 8. The optimum collector area that can cover 1 kW cooling rate is 5 m². The evacuated-tube collector is the worst collector where it obtains the lowest values of solar fraction.

Regarding the annual system efficiency of each system as defined before, it found that CPC collector system has the highest efficiency with the highest solar fraction as obtained from Fig. 8 and Fig. 12. That is can be expected due to its lower heat loss than other collectors. It has the highest efficiency at the summer season in the case of cooling load with high temperature required of 89 C. For other collectors their efficiency for the cooling load is relatively zero. That is very surprising result, the CPC is the most efficient collector when it used only for cooling.

As indicated in the figures 9 to 12, the solar system has the worst efficiency during the summer months where the system is used for cooling. That can understood due to high

heating temperature required; 94 °C required for absorption cooling where it is only 60 °C required for the heating process during the cold months. Perhaps the system efficiency during the autumn months is better than that during the winter and spring. That is because the ambient temperature is low during these periods. For the evacuated-tube collector shown in Fig. 11 the system efficiency is vanished due to zero output of the solar system during the summer season for the cooling load.

Figure 13 presents the hourly efficiency of the system using the flat-plate collector during a year. It is observed clearly that the system efficiency is very low during the cooling season with high temperature required. It equals zero for many days during this period of time. That obtains a very important fact that if we use the system only for the cooling season we must use the CPC collector. In that time the low life-cycle savings are in questionnaire.

Environmental Impact

The environmental impact of the using such system is studied. Mazzarella and Menard (1996) stated different quantities of air and water pollutants for each component of solar system manufacturing and for each kWh of corresponding energy produced by the boiler. Therefore, based on this study the quantities different pollutants are calculated as presented in Fig. 14. Using of solar systems produces lower values of pollutants than the boilers. A significant difference of CO₂ is clearly explained between the solar system and boiler. Where the boiler produces about 3000 ton of CO₂ the solar system production of it can be ignored. Eliminating or treatment of that pollutants cost a lot of money, they can meet the high initial cost of the solar systems.

CONCLUSION

An optimized solar system was used for heating and cooling purposes by both heat pump and single-effect absorption cycle respectively. The system is optimized based on the highest life-cycle savings. The absorption cycle is optimized for the summer season based on weather data. Different solar collectors were compared economically. It is found that flat-plate collectors are more economic where CPC is more efficient. If the system is used only for cooling the CPC collector must be used. The environmental impact of using such systems was estimated. Reduction of air pollution from CO₂ is the significant advantage of utilizing the solar energy.

REFERENCES

1. Assilzadeh F., Kalogirou S.A., Ali Y., Sopian K., "Simulation and optimization of a LiBr solar absorption cooling system with evacuated tube collectors", *Renewable Energy* 30, pp 1143–1159, (2005).
2. Balghouthi M., Chahbani M. H., Guizani A., "Solar Powered air conditioning as a solution to reduce environmental pollution in Tunisia", *Desalination* 185, pp 105–110, (2005).
3. Duffie J. A., Beckman W. A., *Solar engineering of thermal processes*, John Wiley and Sons Inc., (1991).

4. Florides G. A., Kalofirous S. A., Tassou S. A., Wrobel L. C., "Modeling and Simulation of an Absorption Solar Cooling System for Cyprus", *Solar Energy* 72, No. 1, pp. 43–51, (2002).
5. Hewett R., "DOE solar process heat program: FY 1991 solar process heat prefeasibility studies activity", Joint Solar Engineering Conference, ASME, pp 339-342, (1993).
6. Gordon J. M., Rabl A., "Design, analysis and optimization of solar industrial process heat plants without storage", *Solar Energy* 28, No. 6, pp 519-530, (1982).
7. Li Z.F., Sumathy K., "Technology development in the solar absorption air-conditioning systems", *Renewable and Sustainable Energy Reviews* 4, pp 267-293, (2000).
8. Mazzarella L. and Menard M., "Environmental Assessment of Large-scale Solar Heating System", EURO SUN'96 Proceedings, Spt. 16-20, Freiburg, Germany, (1996).
9. Romero R.J., Rivera W., Best R., "Comparison of the theoretical performance of a solar air conditioning system operating with water/lithium bromide and an aqueous ternary hydroxide", *Solar Energy Materials & Solar Cells* 63, pp 387-399, (2000).
10. Syed A., Izquierdo M., Rodríguez P., Maidment G., Missenden J., Lecuona A., Tozer R., "A novel experimental investigation of a solar cooling system in Madrid", *International Journal of Refrigeration* 28, pp 859–871, (2005).
11. TRNSYS Coordinator. A Transient System Simulation Program. Madison: University of Wisconsin, (2000).
12. Tsoutsos T., Anagnostou J., Pritchard C., Karagiorgas M., Agoris D., "Solar cooling technologies in Greece. An economic viability analysis", *Applied Thermal Engineering* 23, pp 1427–1439, (2003).
13. Yang R. U., Wang, "A Simulation Study of Performance Evaluation of Single-Glazed and Double-Glazed Collectors/Regenerators for an Open-Cycle Absorption Solar Cooling System", *Solar Energy* 71, No. 4, pp. 263–268, (2001).

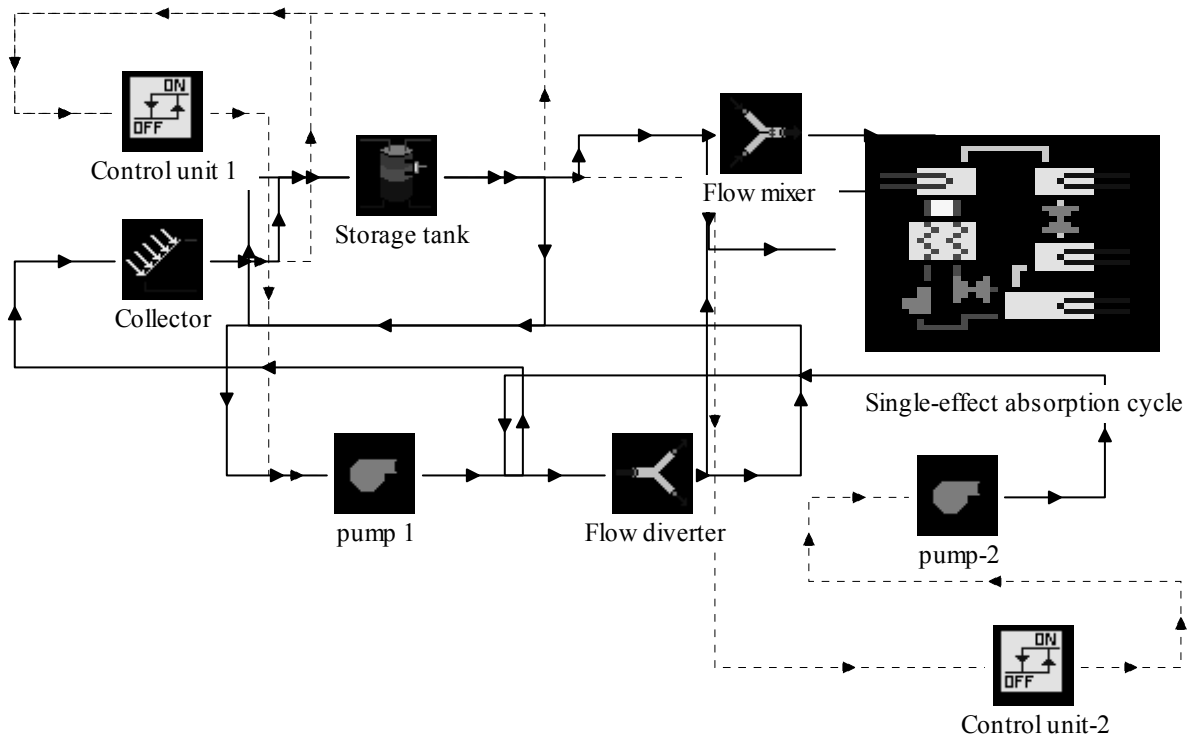


Fig. 1: Schematic diagram of the solar absorption system.

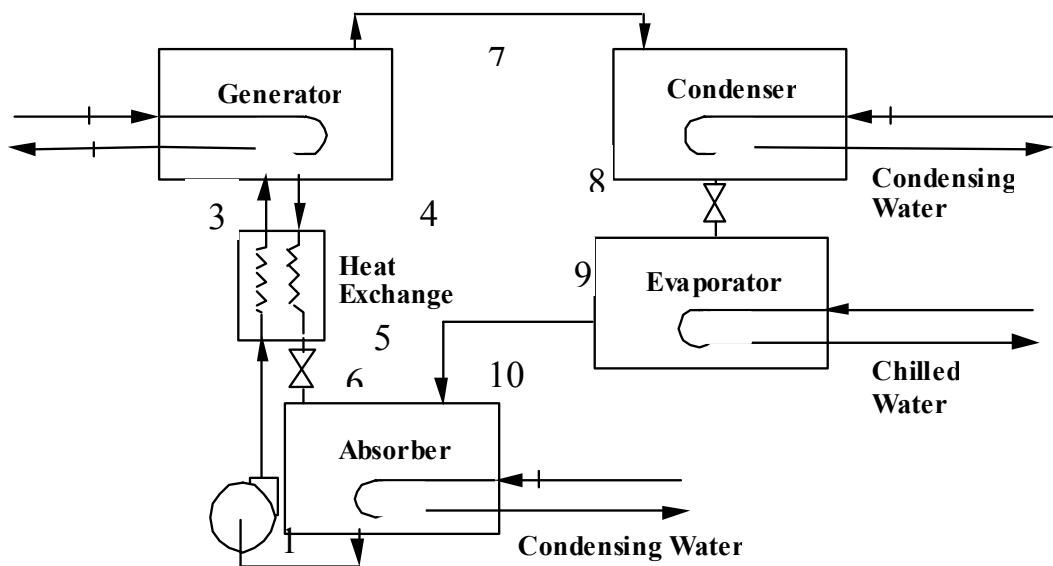


Fig. 2. Schematic diagram of a single-effect absorption refrigeration system

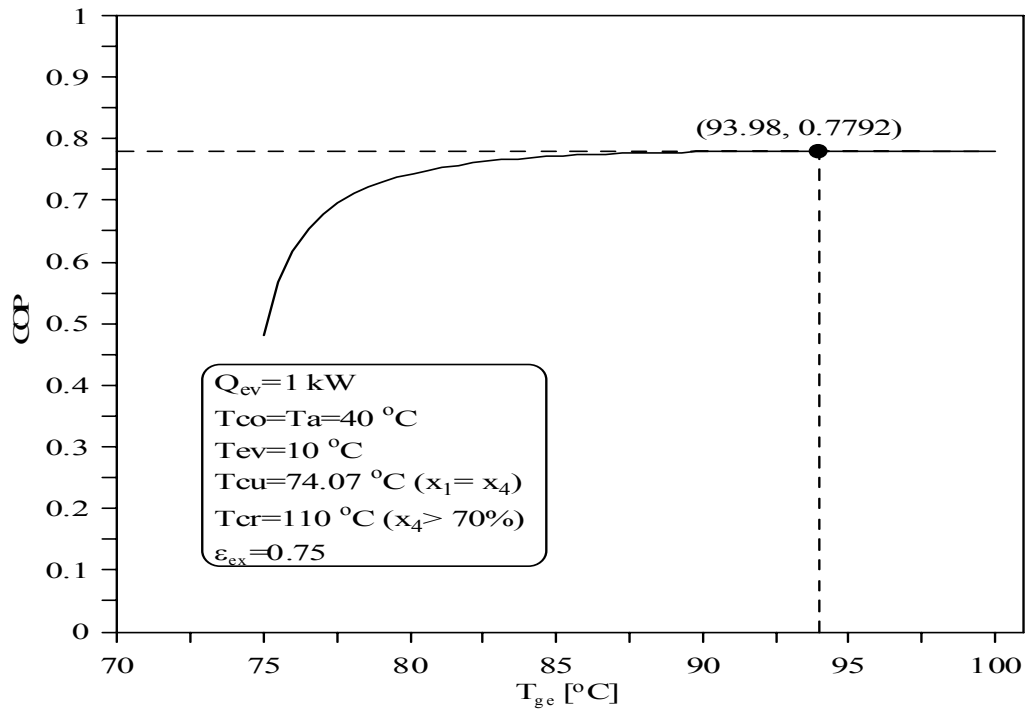


Fig. 3. COP vs. generator temperature for H₂O-LiBr solution.

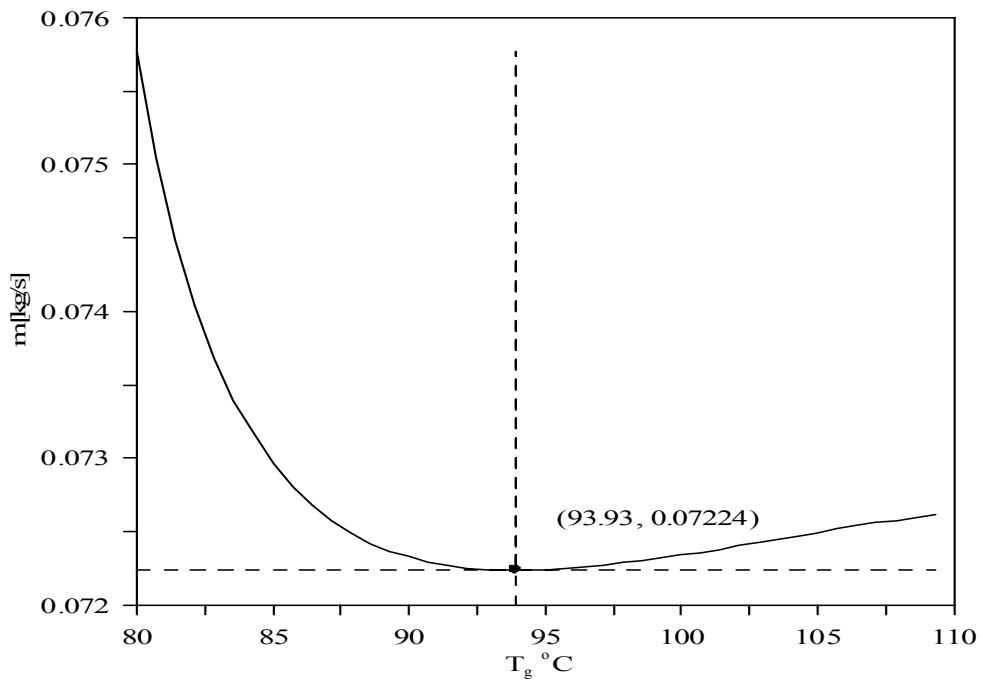


Fig. 4. Heat source mass flow rate vs. generator temperature for H₂O-LiBr solution

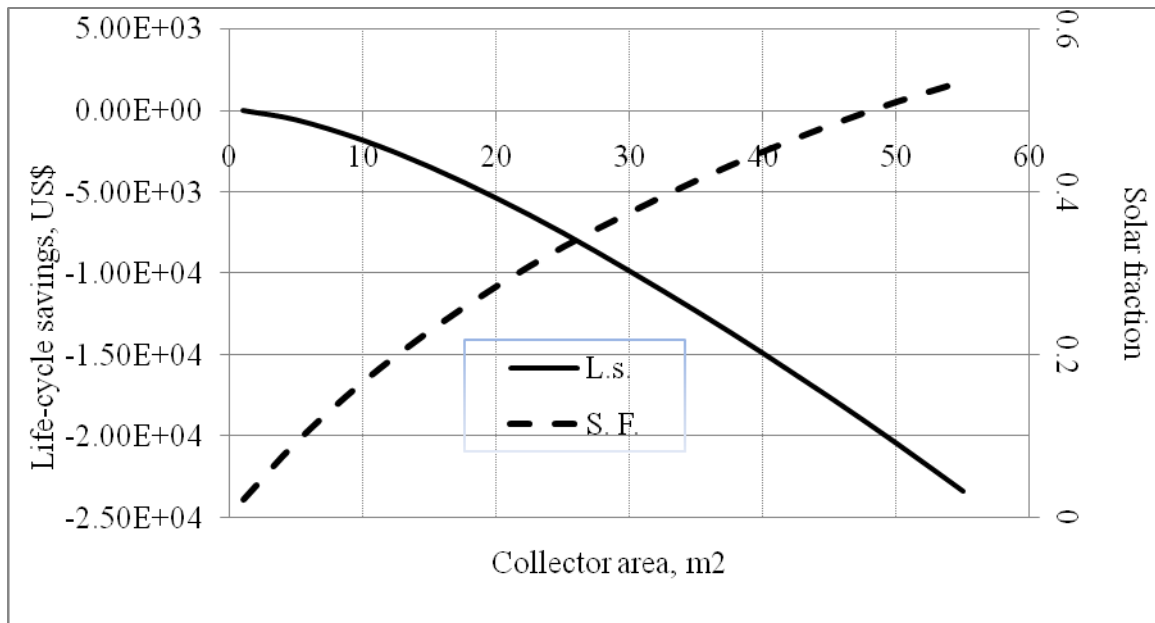


Fig. 5. Economical optimization of parabolic trough collector area.

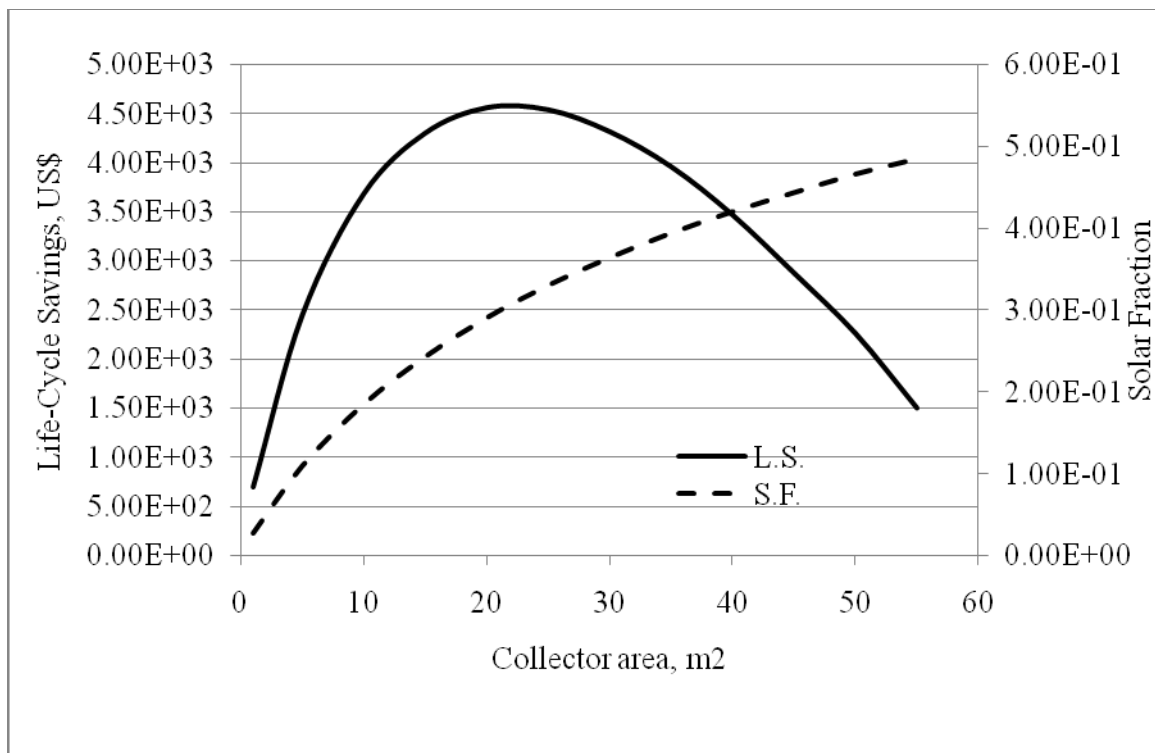


Fig. 6. Economical optimization of flat-plate collector area

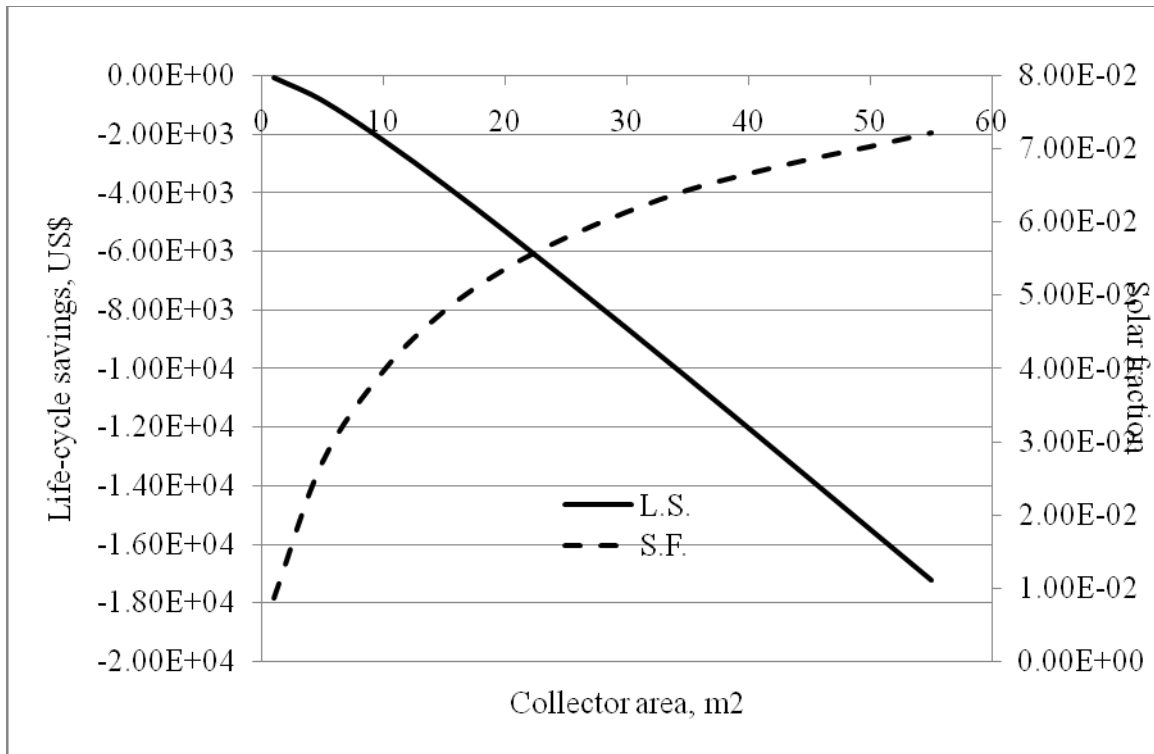


Fig. 7. Economical optimization of evacuated-tube collector area.

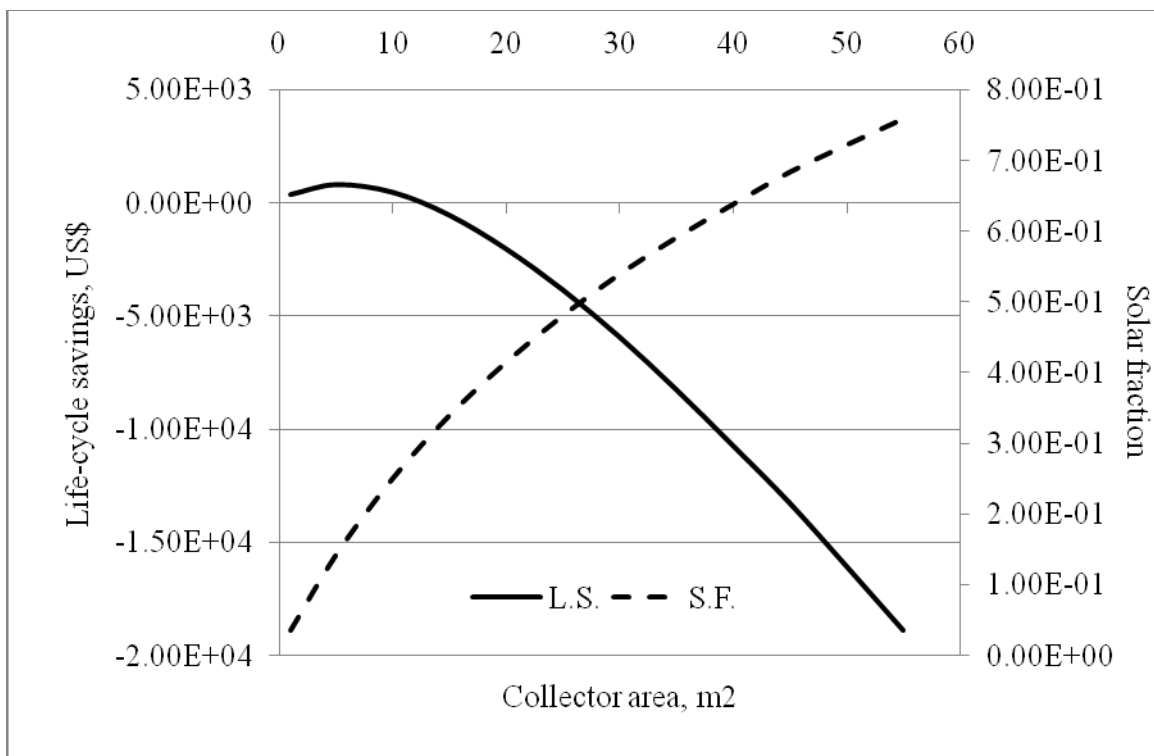


Fig. 8. Economical optimization of CPC collector area

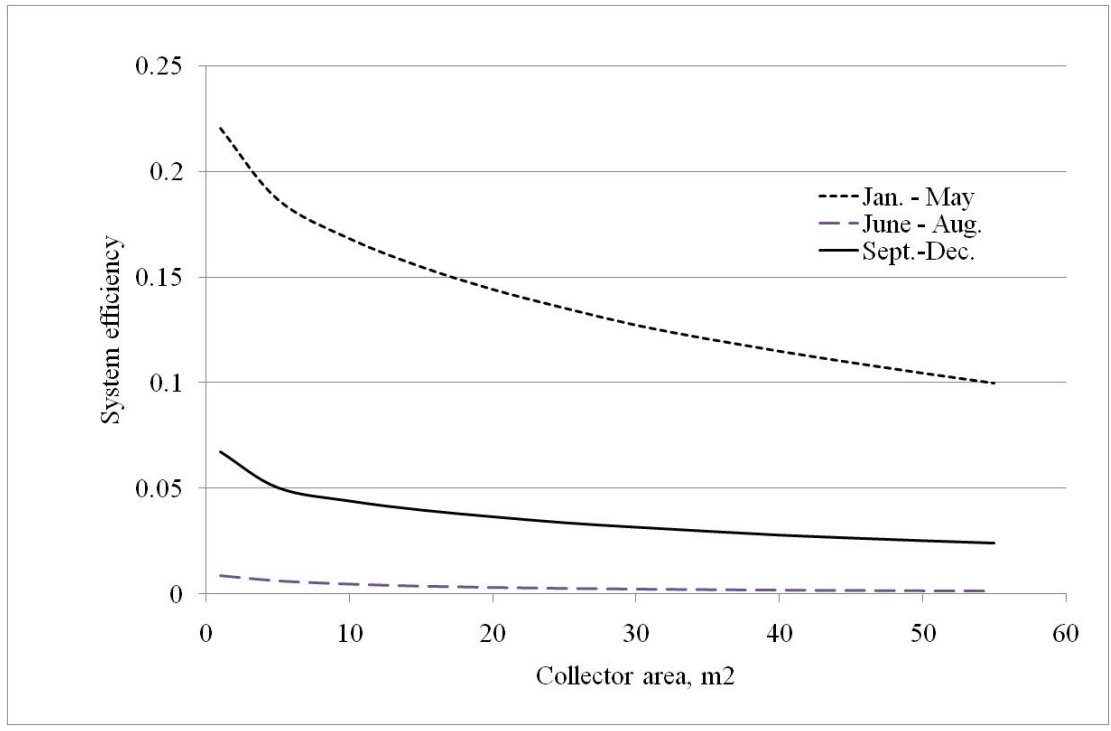


Fig. 9. Solar system performance of parabolic trough collector for cooling and heating processes.

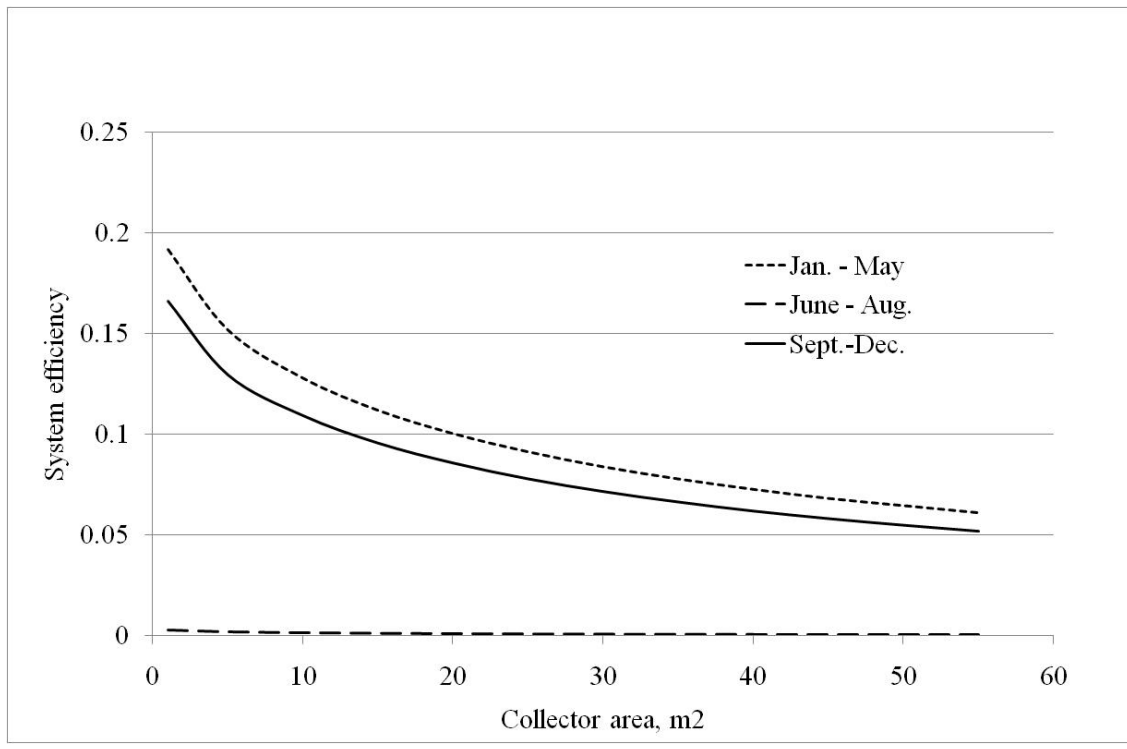


Fig. 10. Solar system performance of flat-plate collector for cooling and heating processes

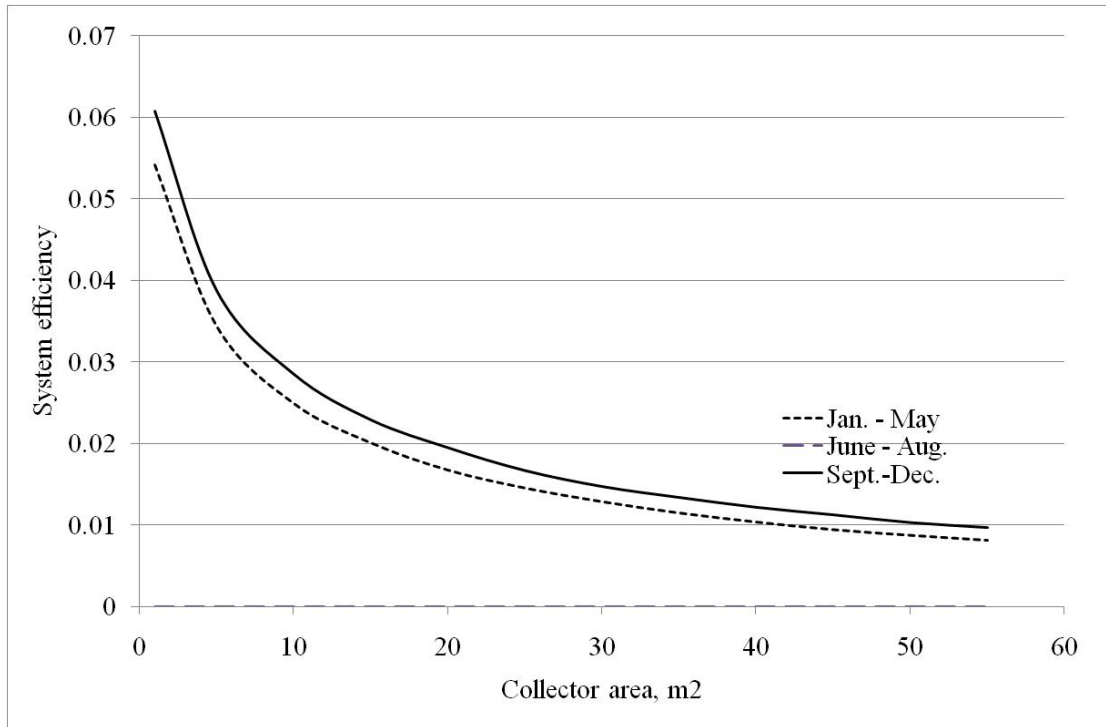


Fig. 11. Solar system performance of evacuated-tube collector for cooling and heating processes.

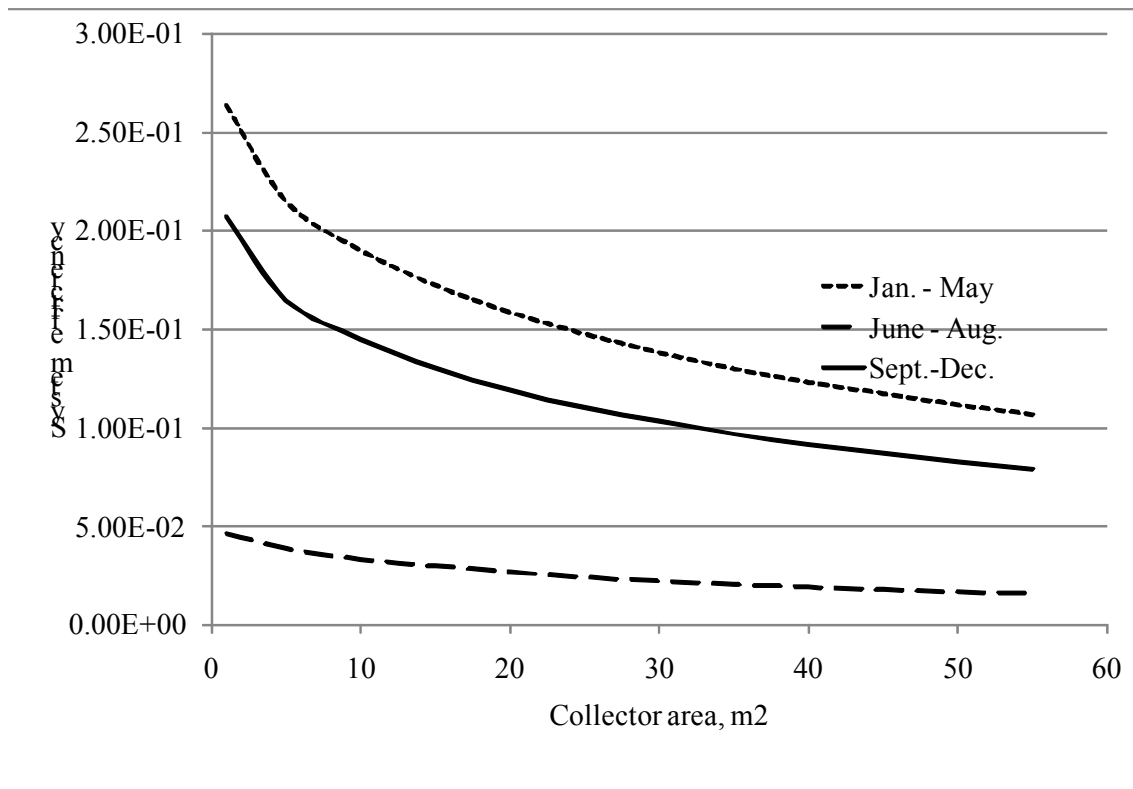


Fig. 12. Solar system performance of CPC collector for cooling and heating processes

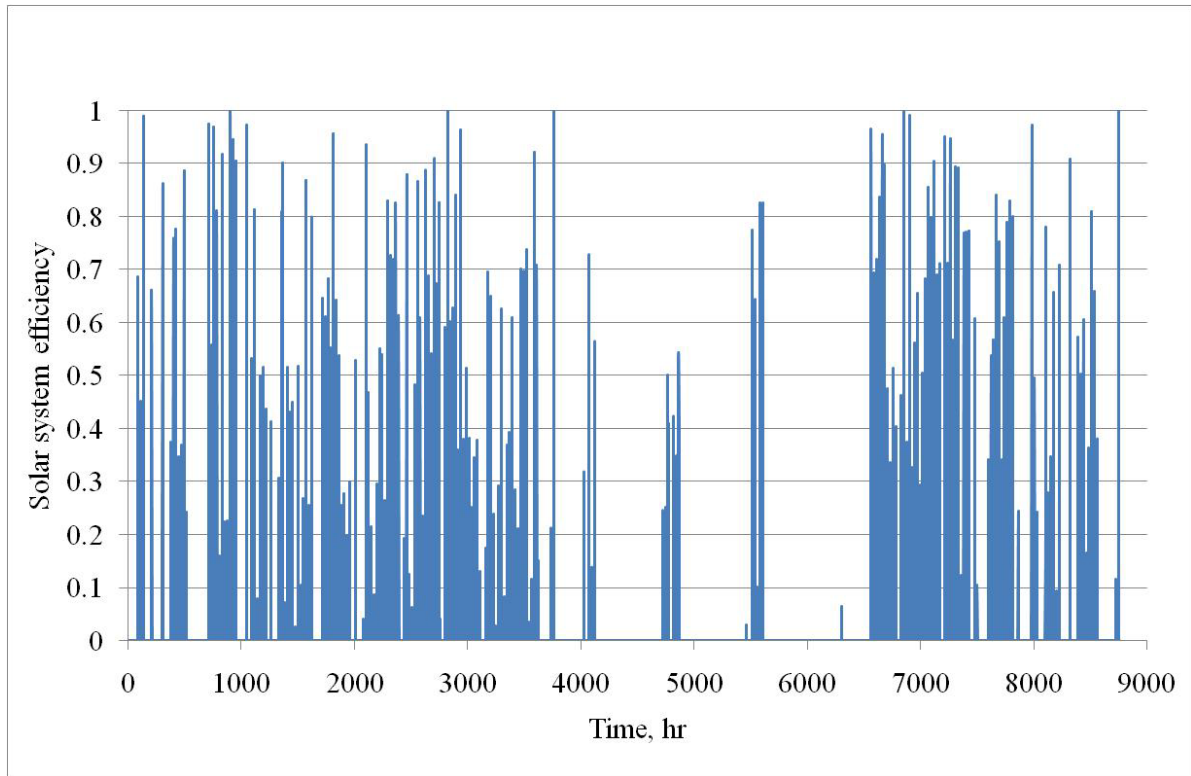


Fig. 13. Annual performance of the flat-plate collector at optimal collector area for heating and cooling loads.

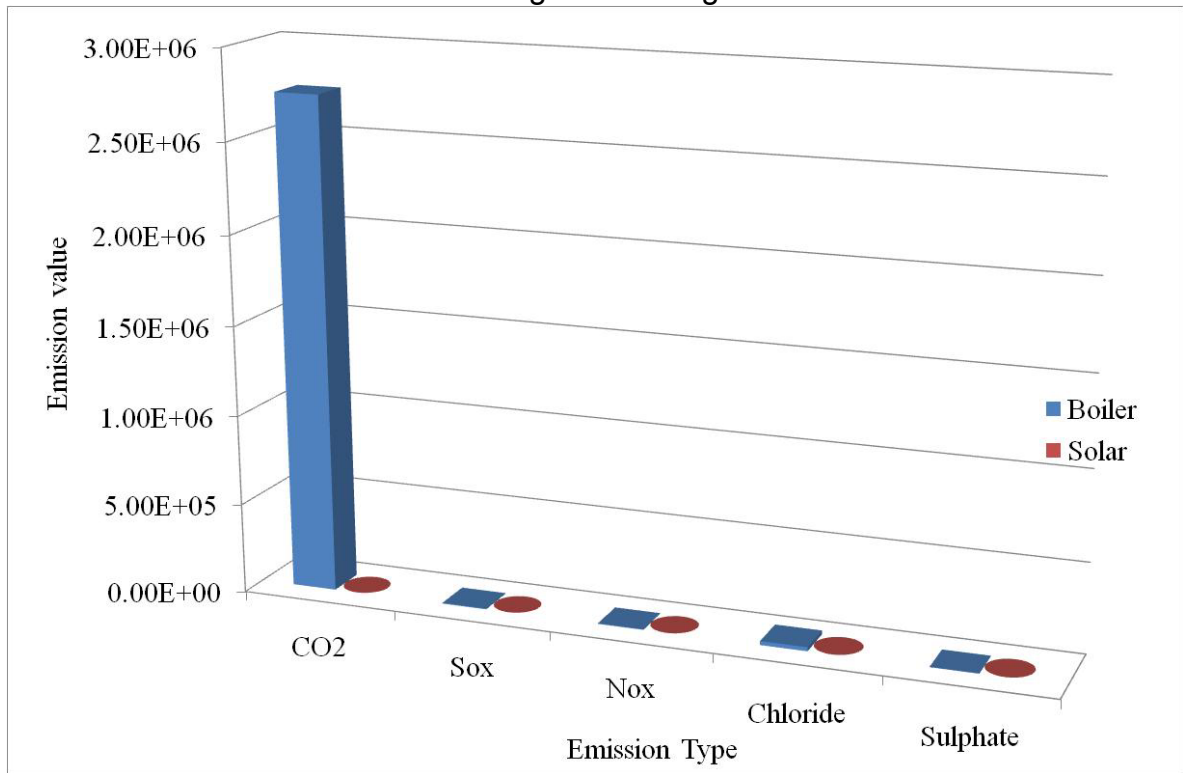


Fig. 14. Environmental Impact of using the solar energy system